

Detection of TeV Gamma-Ray Emission from the Cygnus Region of the Galaxy with Milagro Using a New Background Rejection Technique

A. A. Abdo for the Milagro Collaboration

Michigan State University, Dept. of Physics and Astronomy, East Lansing, MI, 48824

Abstract. Milagro is a TeV gamma-ray observatory that utilizes a large water Cherenkov detector to observe extensive air showers (EAS) produced by high energy particles impacting the Earth's atmosphere. Milagro's distinct advantage compared to other TeV gamma-ray detectors is that it views a wide field (2 steradian overhead sky) and it continuously operates ($> 90\%$ live time). These factors give Milagro the potential for discovery of new sources with unknown positions and times, such as gamma-ray bursts, flaring AGNs, and observation of diffuse and extended sources like the Galactic plane or large supernova remnants. Here we present a new technique for improving background rejection in Milagro as well as a gamma-ray image of the Cygnus region at energies near 12.5 TeV. We report the detection of both an extended source and a large area of diffuse gamma-ray emission from this region of the galaxy. This new extended source has an extent of 0.32 ± 0.12 degrees and an integral flux above 12.5 TeV of $(1.71 \pm 0.24_{stat} \pm 0.34_{sys}) \times 10^{-13} \text{ cm}^{-2} \text{ s}^{-1}$ assuming a differential source spectrum of $E^{-2.6}$. The best-fit location for the source is RA= $304.66 \pm 0.13_{stat} \pm 0.25_{sys}$ degrees and declination $36.96 \pm 0.08_{stat} \pm 0.2_{sys}$ degrees.

Keywords: gamma-ray astronomy; extensive air-shower detectors; cosmic-ray detectors

PACS: 95.55.Ka; 95.55.Ka; 95.85.Pw; 98.70.Rz

1. INTRODUCTION

Milagro is a water-Cherenkov detector at an altitude of 2650m capable of continuously monitoring the overhead sky. The Milagro detector is composed of a central 80m x 60m x 8m (depth) pond with a sparse 200m x 200m array of 175 "outrigger" tanks surrounding it. The central pond is instrumented by 723 photo multiplier tubes (PMTs) that are submerged in 24 million liters of purified water which acts as the detection medium for the secondary particles in an air shower. The 723 PMTs are split into two layers: the top "air shower" layer consists of 450 PMTs and is under 1.4m of water, and the bottom "muon" layer has 175 PMTs and is located 6m under the surface of the water. The shallow depth of the air shower layer allows the accurate measurement of shower particles' arrival times used for direction reconstruction and triggering. The greater depth of the muon layer is used to detect penetrating muons and hadrons which are mostly presented in hadronic air showers. The outrigger array extends the physical area of Milagro from 5000m^2 to $40,000\text{m}^2$, thus improving the core location and angular resolution of the detector by providing a longer lever arm with which to reconstruct events. The angular resolution improves from 1.05° to 0.72° when outriggers are used in the reconstruction.

1.1. Identification and Rejection of Hadronic Events

It is well known that extensive air showers induced by hadronic cosmic rays contain many more muons (from pion decay) and hadrons than EAS induced by gamma rays of comparable energies. The atmospheric overburden at the Milagro site is 20.5 radiation lengths and 8.3 interaction lengths. The muon layer in Milagro is located under 6m of water (corresponding to 17 more radiation lengths and 7.2 interaction lengths). This means that most EM charged particles that enter the pond get absorbed before reaching this layer. On the other hand, muons with energies as low as 1.2 GeV can penetrate and shower near the PMTs of the muon layer. These penetrating muons and hadrons will result in bright compact clusters of light in this layer. Using Monte Carlo simulations we estimate that 79% of all proton showers that trigger Milagro contain a muon and/or a hadron that enters the pond, while only 6% of gamma ray induced air showers contain a muon and/or a hadron that enters the pond.

A new parameter has been developed to parametrize the ‘‘clumpiness’’ in the muon layer. This parameter, A_4 , is given by:

$$A_4 = \frac{(f_{Top} + f_{Out}) \times n_{Fit}}{mxPE} \quad (1)$$

where

- f_{Top} is the fraction of the air shower layer PMTs hit in an event.¹
- f_{Out} is the fraction of the outriggers hit in an event.²
- n_{Fit} is the number of PMTs that entered in the angle fit.
- $mxPE$ is the number of photoelectrons (PEs) in the muon layer PMT with the highest hit.

The first part in the numerator of A_4 carries information about the size of the shower, while n_{Fit} carries information about how well the shower was reconstructed. $mxPE$ carries information about the clumpiness in the muon layer.

Figure 1 shows A_4 distribution for gamma Monte Carlo, proton Monte Carlo, and data. We see a clear difference between the Monte Carlo gamma ray showers and the proton showers, while there is a good agreement between the data and the proton Monte Carlo. Figure 2 shows the efficiencies for retaining data, proton Monte Carlo, and gamma Monte Carlo as a function of A_4 .

The relative increase in the significance of a signal for a given selection criterion is given by the Quality factor (Q) of the cut. For a large number of events, Q is given by:

$$Q = \frac{\epsilon_s}{\sqrt{\epsilon_b}} \quad (2)$$

¹ $f_{Top} = \frac{n_{Top}}{450}$, where n_{Top} is the number of air shower PMTs hit in an event

² $f_{Out} = \frac{n_{Out}}{175}$, where n_{Out} is the number of outriggers hit in an event

Where ϵ_s and ϵ_b are the efficiencies for retaining the signal and background events, respectively.

Figure 3 shows the Q-factor as a function of the minimum value of A_4 required to retain an event. Requiring events to have $A_4 \geq 3.0$ and $nFit \geq 40$ rejects 97.3% of the simulated proton induced air showers that trigger Milagro and 98.4% of the data (for this data sample), and retains 35% of the gamma-ray induced air showers. This results in a predicted Q-factor of 2.2 comparing Monte Carlo proton events to Monte Carlo gamma-ray events, and 2.7 comparing the data to Monte Carlo gamma-ray events.

1.2. Tests of A_4 on the Crab Nebula

The Crab Nebula acts as a standard candle for gamma-ray astronomy due to its long-term, unchanging energy emission through many wavelengths. Figure 4 shows a map of the statistical significance around the Crab Nebula with the $A_4 \geq 3.0$ and $nFit \geq 40$ cuts applied for 1.7 years of data. In this map the Crab Nebula is seen at 8.02σ . Figure 5 shows a map of the statistical significance around the same region for a harder A_4 cut of 12 and $nFit \geq 40$. The Crab Nebula is seen at 5.58σ . Although there was a $\approx 30\%$ loss in statistical significance of the Crab Nebula when the harder A_4 cut was applied, the main advantage of applying this cut is the higher S/B ratio (60.00%) achieved with this cut compared to that with the soft A_4 cut (3.42 %).

1.3. γ -Hadron Relative Weighting

The fact that one can achieve a higher S/B ratios with no major loss in statistical significance when applying harder A_4 cuts led to the development of an alternative analysis method that weights events based on the relative probability that the event was due to a gamma-ray. Events with large A_4 values are assigned high weights, while events with low A_4 are assigned lower weights. Application of this method increases sensitivity by a factor of $\approx 30\%$. Figure 6 shows a map of the statistical significance around the Crab Nebula for the same data set as in figures 3 and 4 with the new analysis method applied. The statistical significance of the Crab Nebula in this map is 10.55σ . The median energy for gamma ray events with this new analysis method is around 12.5 TeV. The angular resolution improves from 0.72° to 0.3° when this method is used.

2. SURVEYING THE TEV GAMMA-RAY SKY

The new weighting analysis method was applied on 5.4 years of data, starting on July 20th 2000 and ending on March 2nd 2006. In total, 1914.56 days of on-time data were included. Sources are only observable as they transit through Milagro's field of view (FOV), so a day of data represents approximately 4-6 hours of exposure for any given northern hemisphere source. Figure 7 shows the northern hemisphere as viewed in TeV gamma-rays. The most prominent feature of this map is the Galactic ridge spanning

declinations 0 to 50 degrees and right ascensions 285 to 320 degrees. The Crab Nebula is visible in this map at 14 standard deviations³.

2.1. Cygnus Region of the Galactic Plane

The Cygnus region is the most luminous source of High Energy gamma rays in the northern sky at energies between 30MeV and 100 GeV as reported by EGRET[1]. High Energy gamma-ray emission from this region is complex and is likely due to the combination of both diffuse and point sources. A large contribution to the VHE emission must come from the interaction of cosmic rays with the relatively dense matter distribution in the region. The HEGRA experiment has detected a localized unidentified TeV source in the Cygnus region with flux of 30 mCrab[2]. A previous Milagro measurement[3] of the diffuse flux from the Galactic longitude region 40 - 100 degrees, normalized to the EGRET measurements in the same region, showed an excess in the region near Galactic longitude 80 degrees - the Cygnus region of the Galaxy[4].

Figure 8 shows the Cygnus region in Galactic coordinates. The contours on the figure show the EGRET model for the diffuse gamma ray emission in the region. At 12 standard deviations this is the second brightest region of TeV emission (after the Crab Nebula) in the northern hemisphere. The crosses in the figure show the location and location error of the EGRET sources in this region (none of which have been definitively identified with counterparts at other wavelengths). While the average angular resolution of Milagro for a single gamma ray is 0.5 degrees, the highest energy gamma rays detected have substantially better angular resolution (0.3 degrees) and background rejection. An examination of the arrival directions of the higher-energy photons shows that this source is most likely an extended source of TeV gamma rays. This new extended source has an extent of 0.32 ± 0.12 degrees and an integral flux above 12.5 TeV of $(1.71 \pm 0.24_{stat} \pm 0.34_{sys}) \times 10^{-13} cm^{-2} s^{-1}$ assuming a differential source spectrum of $E^{-2.6}$. The best-fit location for the source is RA= $304.66 \pm 0.13_{stat} \pm 0.25_{sys}$ degrees and declination $36.96 \pm 0.08_{stat} \pm 0.2_{sys}$ degrees.

ACKNOWLEDGMENTS

We acknowledge Scott Delay and Michael Schneider for their dedicated efforts in the construction and maintenance of the Milagro experiment. This work has been supported by the National Science Foundation, the US Department of Energy, Los Alamos National Laboratory, the University of California, and the Institute of Geophysics and Planetary Physics.

³ The significance of the Crab Nebula on the 5.4 years is less than what one may expect by scaling the significance from the 1.7 years data set, namely $10.55 \times \sqrt{5.4/1.7} = 18.8$. This is due to the fact the larger data set contains data with lower quality (no outriggers) than the 1.7 years data set.

REFERENCES

1. Hartman R.C., Bertsch D.L., Bloom S.D. et al., *Ap. J. Suppl.* **123**, 79 (1999)
2. Aharonian F. et al., *Astron. and Astrophys.* **431**, 197 (2005)
3. Atkins. R.A., et al., *phys. rev. Lett.* **95**, id. 251103 (2005)
4. Hunter, S.D. et al., *Astrophys. J.* **481**, 205-240 (1997)
5. Atkins. R.A., et al., *Astrophys. J.* **595**, 803-811 (2003)

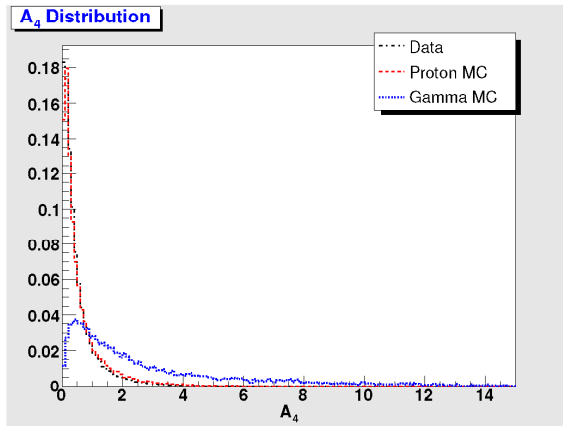


FIGURE 1. Distribution of A₄ for gamma Monte Carlo, proton Monte Carlo, and data.

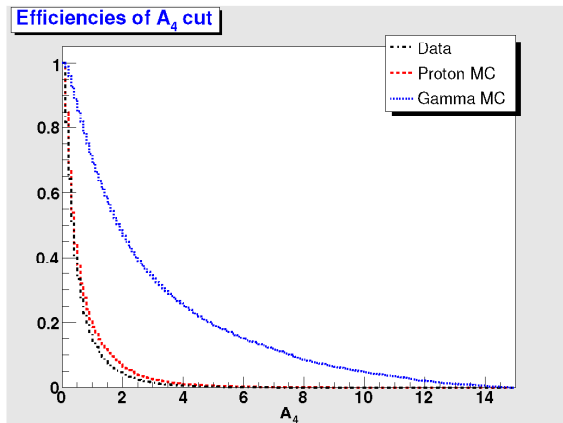


FIGURE 2. Efficiencies for retaining data, proton Monte Carlo, and gamma Monte Carlo as a function of A₄.

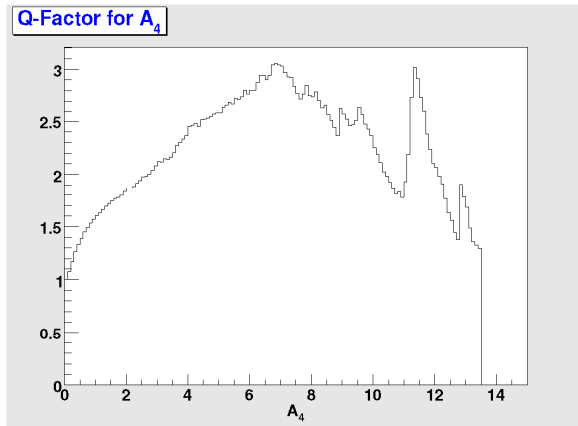


FIGURE 3. Q-factor as a function of the minimum value of A_4 required to retain an event.

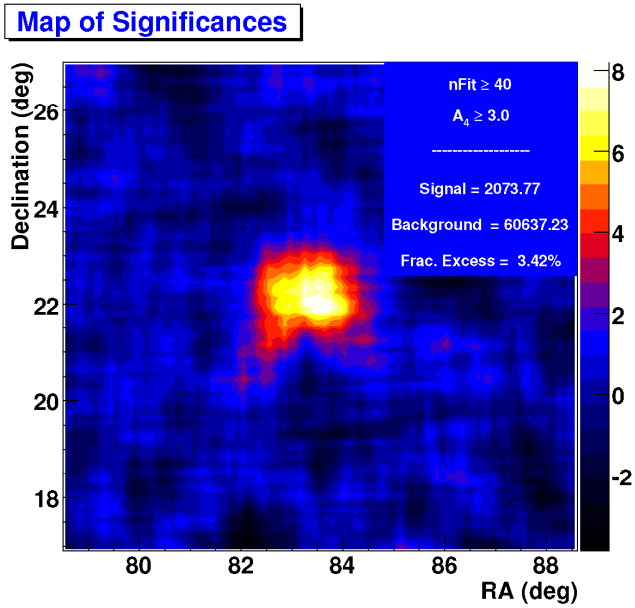


FIGURE 4. Map of the statistical significance around the Crab Nebula with the $A_4 \geq 3.0$ and $nFit \geq 40$ cuts applied.

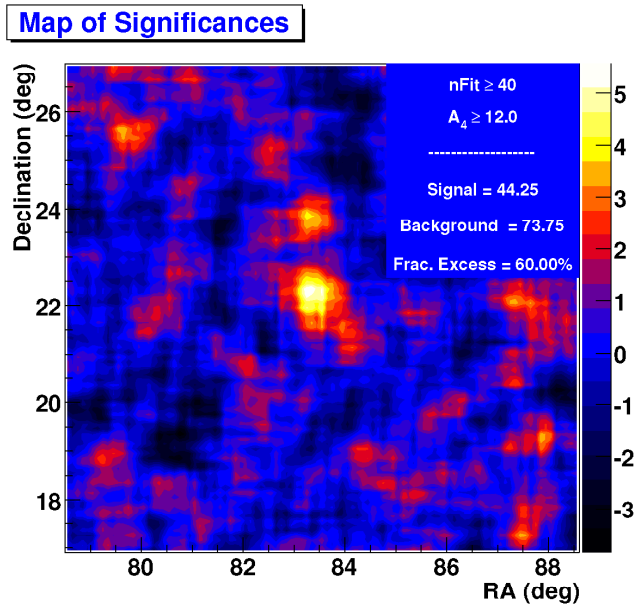


FIGURE 5. Map of the statistical significance around the Crab Nebula with the $A_4 \geq 12.0$ and $nFit \geq 40$ cuts applied.

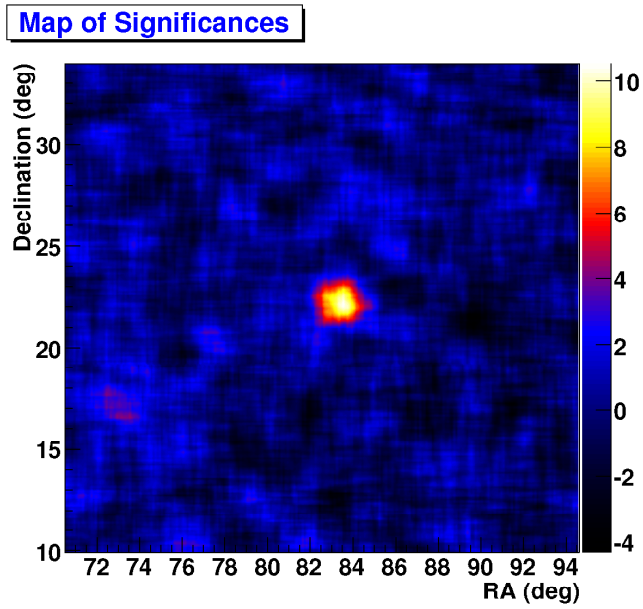


FIGURE 6. Map of the statistical significance around the Crab Nebula with the new γ -Hadron weighting analysis method applied.

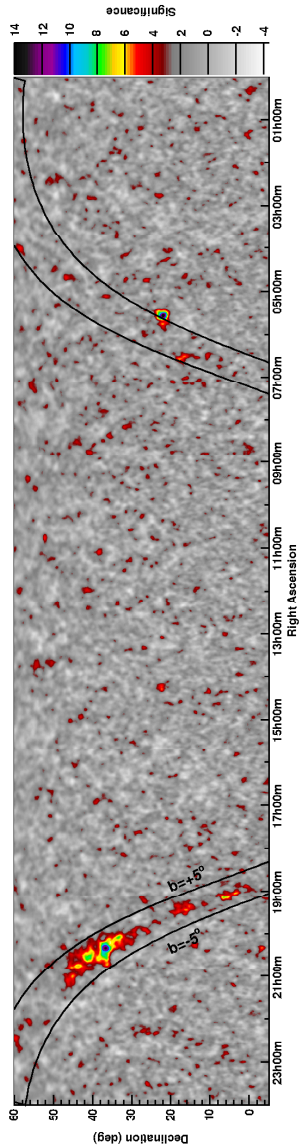


FIGURE 7. The northern hemisphere in TeV gamma rays. This figure shows the statistical significance of the observed excess (or deficit) at each point in the sky (points below 2 standard deviation have been suppressed for clarity). The Galactic ridge is clearly visible in this map. The Cygnus Region is within this ridge near a declination of 37 degrees. The Crab Nebula is the most significant TeV gamma ray source in the northern hemisphere (R.A. 5h 44m and declination 22 degrees), seen here at 14σ . The dark lines mark a ± 5 degree region around the Galactic plane.

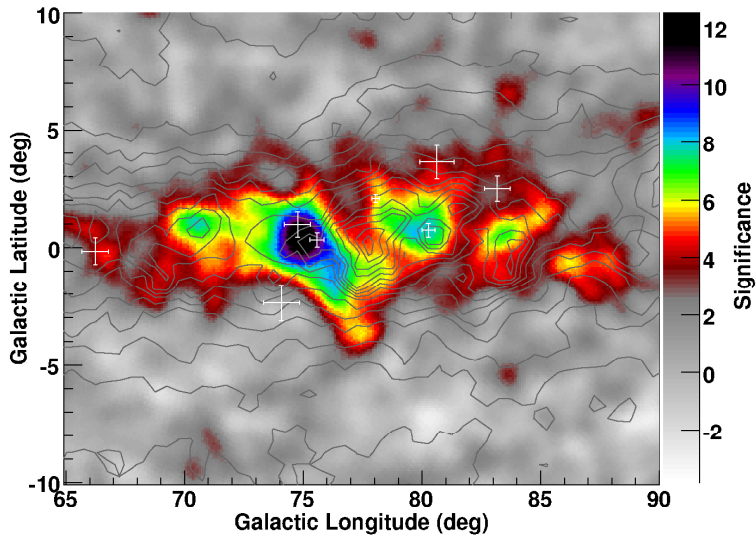


FIGURE 8. The Cygnus Region of the Galaxy as seen in TeV gamma rays. This figure shows the statistical significance of the observed excess (or deficit) at each point in the sky (points below 2 standard deviation have been suppressed for clarity). Superimposed on the image are contours showing the EGRET diffuse gamma-ray emission model for this region of the Galaxy. There is a good correlation between the TeV emission and the EGRET model. The white crosses show the location of the EGRET sources and their corresponding location errors.